Nucleus-Carrier Interactions in the Group V Semimetals: Dependence on Temperature and Pressure *

J. M. Keartland, I. P. Goudemond, G. C. K. Fölscher, and M. J. R. Hoch

Condensed Matter Physics Research Unit, Physics Department, University of the Witwatersrand, Johannesburg, South Africa

Z. Naturforsch. **47a**, 49–53 (1992); received August 27, 1991

A review is given of pulsed NQR spin-lattice relaxation measurements on the rhombohedral semimetals, arsenic (As) and antimony (Sb). The nuclear spin-lattice relaxation time T_1 has been measured in the temperature range 100 mK–600 K. The data follow the Korringa relation at low temperatures, but deviations from this relation are found as the temperature is increased. The results are quantitatively explained by considering interactions of the nuclei with the carriers at the Fermi surface. Above the Debye temperature (θ_D) the data may be understood by including a two phonon process in the analysis. The relaxation data for As and Sb are found to scale with θ_D. T_1 has been measured for As at 295 K in the pressure range 0–10 kbar. The results are discussed in terms of changes in the Fermi surface parameters.

PACS numbers: 76.60.Es; 76.60Gv; 71.20Cf.

Key words: Semimetals, Pulsed NQR, Nucleus-carrier interactions, Nucleus-phonon interactions, Fermi surface parameters.

1. Introduction

The Group V semimetals crystallize in the rhombohedral A_7 structure [1]. This gives rise to an axially symmetric electric field gradient at each nuclear site. The naturally occurring isotopes in these materials have nuclei with large quadrupole moments, and they are ideal candidates for NQR. Measurements of the quadrupole resonance frequencies as a function of temperature and pressure [2–5] have been undertaken by several workers using continuous wave NQR. Pulsed NQR measurements of nuclear spin-lattice relaxation effects [6–9] have shown that nucleus-carrier interactions play an important role at lower temperatures. It has been suggested that nucleus-phonon interactions may make important contributions as the temperature increases [8].

2. Theoretical Considerations

The rate equations describing nuclear spin-lattice relaxation have been derived for $I = \frac{5}{2}$ and $I = \frac{3}{2}$ using a procedure developed by MacLaughlin et al. [10]. For $I = \frac{5}{2}$ the relaxation is governed by two exponentials and a unique T_1 cannot be defined, unless it is assumed that quadrupolar interactions are negligible. The rate equation for $I = \frac{3}{2}$ is governed by a single exponential and T_1 can be defined, in terms of magnetic (W_m) and quadrupolar (W_{Q1}, W_{Q2}) transition rates as follows:

$$\frac{1}{T_1} = 6\,W_m + 24\,W_{Q1} + 12\,W_{Q2}. \quad (1)$$

The quantities W_m, W_{Q1}, and W_{Q2} have been calculated for interactions of the nucleus with the carriers at the Fermi surface (FS). The Fermi surfaces of As and Sb have been studied experimentally [11–14] and theoretically [15, 16], and may be approximated by ellipsoidal pockets distributed in k-space. The calculations of Mitchell [17] for a spherical FS have been extended to the non-spherical FS of As [18] and Sb [8]. Both contact and non-contact interactions were considered. Using available free atom wavefunctions [19] and measured FS parameters obtained from the literature [13, 14], we calculated the transition rates at 77 K. The results are shown in Table 1. The expression for the dominant magnetic relaxation contribution, the contact term W_m^c, is

$$W_m^c = \frac{2\pi}{\hbar}\left[\frac{\mu_0}{6}\,\mu_B\, g\,\mu_N\, \varrho(E_F)\,|u_k(0)|^2\right]^2 kT, \quad (2)$$

* Presented at the XIth International Symposium on Nuclear Quadrupole Resonance Spectroscopy, London, United Kingdom, July 15–19, 1991.

Reprint requests to Prof. Dr. M. J. R. Hoch, Physics Department, University of the Witwatersrand, P.O. Wits 2050, Johannesburg, South Africa.

0932-0784 / 92 / 0100-0049 $ 01.30/0. – Please order a reprint rather than making your own copy.

Table 1. Nucleus-carrier transition rates at 77 K calculated using atomic wavefunctions. The results for the quadrupolar contributions include Sternheimer antishielding effects. The values for the non-contact terms are believed to be considerably underestimated. This is discussed in the text.

		W_m^c (s^{-1})	W_m^{nc} ($10^{-7}s^{-1}$)	W_{Q1} ($10^{-8}s^{-1}$)	W_{Q2} ($10^{-8}s^{-1}$)
arsenic	electrons	0.56	3.20	1.35	7.95
	holes	0.98	2.96	10.4	3.69
antimony	electrons	0.73	0.22	0.04	0.28
	holes	1.06	0.57	0.58	0.55

where $\varrho(E_F)$ is the density of states at the FS, and $|u_k(0)|^2$ is the probability density of the carriers at the nucleus. The Knight shift has been estimated using the free atom wavefunctions. Comparing the results with those for Sb obtained using good crystal wavefunctions [20], it is clear that the free atom wavefunctions for the *p*-wave carriers are very different from the crystal wavefunctions. The calculations suggest that the non-contact terms in Table 1 may be underestimated by as much as 10^6.

The interaction of the nucleus with acoustic phonons may also contribute to spin-lattice relaxation. A simple model, that employs the Debye approximation for the phonon density of states, is used to estimate the phonon contribution [21]. The quadrupolar transition rates may be written as

$$W_{Q\mu} = \frac{243\pi}{16}\left[\frac{eQF_\mu\hbar}{I(2I-1)mv^2}\right]^2 \cdot \int_0^{\omega_D} \frac{\exp(\beta\hbar\omega)\omega^6}{[\exp(\beta\hbar\omega)-1]^2\omega_D^6}\,d\omega, \tag{3}$$

where $\beta = 1/kT$, μ takes the values 1 and 2, the quantities F_μ depend on the crystal structure, m is the atomic mass, v is the velocity of sound in the crystal and ω_D is the Debye frequency. The Debye temperature is given by $\hbar\omega_D = k\theta_D$ ($\theta_D = 282$ K for As, $\theta_D = 210$ K for Sb). The integral in (3) may be re-written in order to obtain the temperature dependence of the transition rates as

$$W_{Q1,Q2}(T) \propto T^7 \int_0^{\theta_D/T} \frac{x^6 e^x}{(e^x-1)^2}\,dx. \tag{4}$$

In the high temperature limit $T \geqq \theta_D$ this gives a T^2 dependence for the transition probabilities.

3. Experimental Details

The samples used in the experiments consisted of high purity (99.9995%) material which was crushed to 25 μm before annealing and sealing in ampoules. Relaxation measurements were made with a pulsed NQR spectrometer operating in the range 21–23.5 MHz. Spin-echo methods were necessary, with digital signal averaging used to improve the signal-to-noise ratio.

Low temperature measurements were carried out in an Oxford Model 400 dilution refrigerator ($T < 4$ K) and in a variable temperature helium cryostat ($4\text{ K} \leqq T \leqq 60$ K). At higher temperatures various fixed temperature baths were used, as well as a furnace probe for the highest temperatures.

High pressure experiments were carried out at ambient temperature (295 K) using standard piston-cylinder techniques. The pressure in the sample chamber was monitored using a manganin-resistance gauge, and the sample holder was designed to allow the hydrostatic fluid to permeate throughout the sample.

4. Results and Discussion

A plot of the experimental T_1 data as a function of reduced temperature, T/θ_D, is shown in Figure 1. T_1 for As is defined in (2), and the results for Sb have been obtained by assuming that only magnetic interactions contribute to relaxation processes, as discussed in § 2. The expression for T_1 in As may be written in terms of the temperature dependence of the various contributions to spin-lattice relaxation

$$\frac{1}{T_1} = AT + BT^7 \int_0^{\theta_D/T} \frac{x^6 e^x}{(e^x-1)^2}\,dx. \tag{5}$$

The constants A and B in (5) were determined using the following procedure. B is set to zero and A is determined by fitting a straight line to the low temperature ($T \leqq 88$ K) As data. This value for A is substituted into (5) and the value for B determined using a least-squares fitting procedure to the full range of As data points shown in Figure 1. The integral in (5) was determined numerically for each temperature using Simpson's rule. The curves shown in Fig. 1 are the result of this fitting procedure. The Sb data should be analysed in terms of W_m, W_{Q1}, and W_{Q2}. It is clear that the data for As and Sb scale with θ_D, which supports

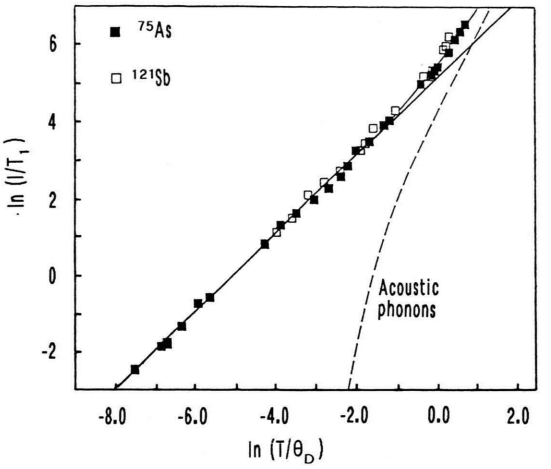

Fig. 1. Spin-lattice relaxation rate, $1/T_1$, as a function of reduced temperature for As and Sb. The curves shown are the result of fitting the theoretical nucleus-carrier and nucleus-phonon models to the As data. The curve through the data points is a result of the fitting procedure described in the text.

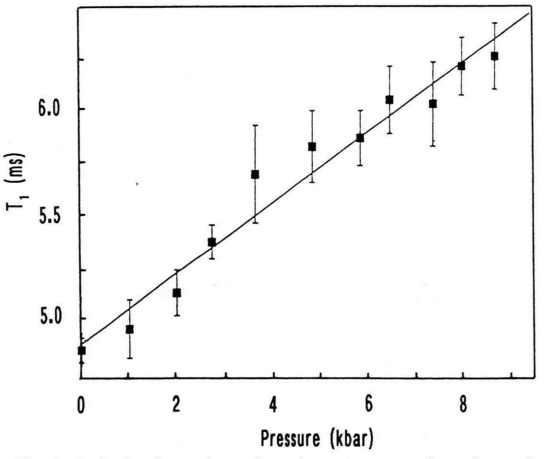

Fig. 2. Spin-lattice relaxation time, T_1, as a function of pressure for As. The error bars shown are the result of a linear regression analysis of the relaxation data. The curve through the data is the best fit straight line, the slope of which is given in the text.

the proposed phonon mechanism. It is interesting, but fortuitous, that the magnitudes of the relaxation rates are so similar when plotted in this way.

The T_1 results for As as a function of pressure are shown in Figure 2. Measurements were made at 295 K over the pressure range 0–10 kbar. The curve shown is the result of a linear regression analysis of the data. The slope of the line is 0.17 ms kbar^{-1}.

In the analysis of the high pressure T_1 results, we assume that both the carrier and phonon contributions change with pressure. It should be noted that the carrier contribution to the total relaxation rate at 295 K and atmospheric pressure is greater than 70%. The pressure variation of the relaxation rate at a constant temperature may be written as

$$\frac{1}{T_1}(P) = \frac{1}{T_1^{\mathrm{C}}}(P) + \frac{1}{T_1^{\mathrm{P}}}(P), \tag{6}$$

where T_1^{C} and T_1^{P} refer to carrier and phonon contributions to the relaxation rate, respectively. We assume that the major contribution to T_1^{C} is due to the contact interaction, in line with the calculations described in § 2. $T_1^{\mathrm{C}}(P)$ may be written in terms of the pressure variation of the density of carrier states at the Fermi level, $\varrho(E_{\mathrm{F}}, P)$, if we assume that the dominant s-wave part of the carrier wavefunction at the nucleus does not change significantly with pressure. This assumption is unavoidable in the absence of good carrier wavefunctions for rhombohedral As. The fact that the free atom wavefunctions are a good approximation to the crystal wavefunctions at the nucleus, as mentioned previously, gives us some confidence in the assumption. The ratio $\dfrac{\varrho(E_{\mathrm{F}}, P)}{\varrho(E_{\mathrm{F}}, 0)}$ may be written as follows in terms of the atomic volume, v_0, the carrier concentration, n, and the average effective mass, $m^* = (m_x m_y m_z)^{1/3}$, if we assume that the electron and hole FS pockets deform uniformly and at the same rate with the application of pressure:

$$\frac{\varrho(E_{\mathrm{F}}, P)}{\varrho(E_{\mathrm{F}}, 0)} = \left[\frac{v_0(P)}{v_0(0)}\right]\left[\frac{n(P)}{n(0)}\right]^{1/3}\left[\frac{m^*(P)}{m^*(0)}\right]. \tag{7}$$

An estimate of changes in the phonon contribution to the spin-lattice relaxation rate with pressure may be made if we assume that the elastic constants do not change significantly with pressure over the range 0–10 kbar. An estimate of $T_1^{\mathrm{P}}(P)$ may be determined from the ratio

$$\frac{T_1^{\mathrm{P}}(P)}{T_1^{\mathrm{P}}(0)} = \frac{W_{\mathrm{Q}}(0)}{W_{\mathrm{Q}}(P)} = \left[\frac{v_0(P)}{v_0(0)}\right]^{3/2} \tag{8}$$

and previous results for $\dfrac{v_0(\mathrm{P})}{v_0(0)}$ [22]. T_1^{P} decreases by approximately 3.9% in the range 0–10 kbar. Plots of $\dfrac{T_1^{\mathrm{C}}(P)}{T_1^{\mathrm{C}}(0)}$ and $\dfrac{T_1^{\mathrm{P}}(P)}{T_1^{\mathrm{P}}(0)}$ are shown in Figure 3. $\dfrac{\varrho(E_{\mathrm{F}}, P)}{\varrho(E_{\mathrm{F}}, 0)}$ and

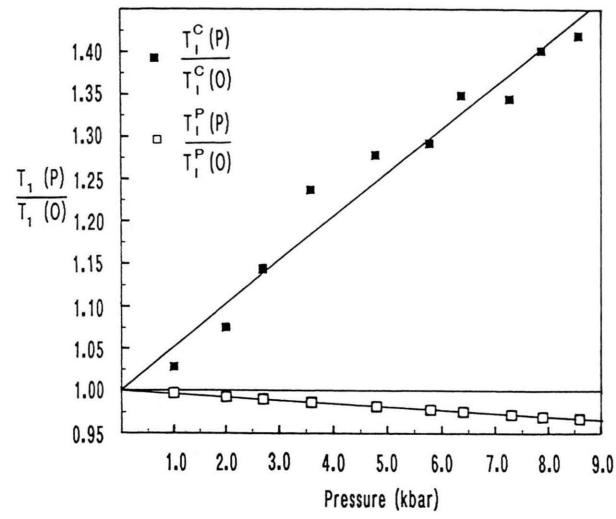

Fig. 3. Variation of $\frac{T_1^C(P)}{T_1^C(0)}$ and $\frac{T_1^P(P)}{T_1^P(0)}$ with pressure. The results for $\frac{T_1^P(P)}{T_1^P(0)}$ were obtained from a calculation based on a simple model described in the text. The $\frac{T_1^C(P)}{T_1^C(0)}$ results are extracted from the experimental data using the results for $\frac{T_1^P(P)}{T_1^P(0)}$. The curves shown are the best fit straight lines through each set of data.

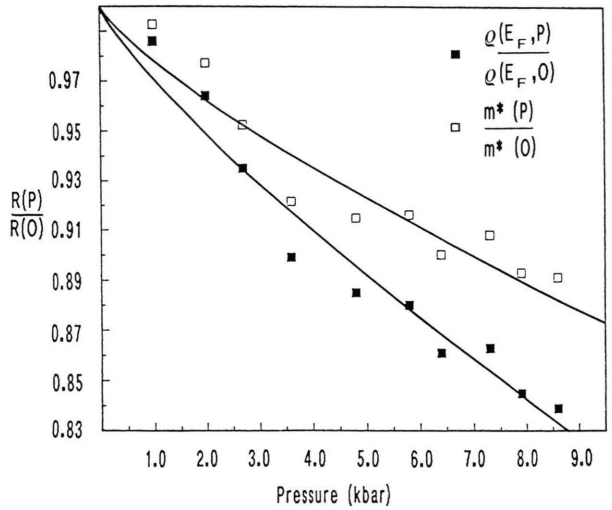

Fig. 4. Variation of $\frac{\varrho(E_F,P)}{\varrho(E_F,0)}$ and $\frac{m^*(P)}{m^*(0)}$ with pressure. The data have been extracted from the results for $\frac{T_1^C(P)}{T_1^C(0)}$, shown in Fig. 3, using equations presented in the text. The curves shown are the result of a least-squares fitting procedure described in the text.

$\frac{m^*(P)}{m^*(0)}$ may then be calculated using previous results for the pressure variation of v_0 [22] and n [23]. The results are displayed in Figure 4. Relations of the form

$$\frac{R(P)}{R(0)} = 1 - \left[\frac{P}{P_0}\right]^{\gamma} \tag{9}$$

were fitted to each set of data, where $R(P)$ represents the relevant quantity (either $\varrho(E_F,P)$ or $m^*(P)$). The exponents γ obtained from least-squares procedures suggest non-linear behaviour. These results may be compared with the carrier concentration measurements of Brandt et al. [23] and Rakhminina [24]. The present results show a qualitative agreement with these measurements in the pressure range investigated. The pseudopotential calculations of Pospelov [25] may be extended to calculate the pressure variation of the FS parameters. The results of such a calculation would provide a useful comparison with the results presented here.

5. Conclusions

Nucleus-carrier interactions play a dominant role in spin-lattice relaxation at temperatures below θ_D in As and Sb. Above θ_D a two phonon process becomes important, and the data for As and Sb scale with θ_D. Theoretical calculations which we have carried out can explain the observed temperature dependence in the low ($T < \theta_D$) and high temperature regimes. Quantitative agreement of theory and experiment is obtained in the temperature range in which Korringa behaviour is observed.

Measurements of T_1 as a function of pressure have allowed us to study pressure-induced changes in the FS of As. The results show qualitative agreement with previous measurements and calculations. NQR may be used to obtain this information in the semimetals up to relatively high pressures using piston-cylinder techniques.

Acknowledgements

The authors gratefully acknowledge the contributions of Dr. I. Sigalas in the design of the pressure cell. P. van der Schyff, H. Brenner, and E. Rood assisted in the construction of the equipment and in certain of the low temperature measurements. Financial support from the Foundation for Research Development is also acknowledged.

[1] R. W. G. Wyckoff, Crystal Structures, John Wiley and Sons, New York 1963.
[2] S. N. Sharma, Phys. Lett. **57 A,** 379 (1976).
[3] T. J. Bastow and H. J. Whitfield, Solid State Commun. **18,** 955 (1976).
[4] T. J. Bastow, R. J. C. Brown, and H. J. Whitfield, Phys. Lett. **78 A,** 198 (1980).
[5] R. R. Hewitt and B. F. Williams, Phys. Rev. **129,** 1188 (1963).
[6] G. E. Jellison, Jr., and P. C. Taylor, Solid State Commun. **27,** 1025 (1978).
[7] R. R. Hewitt and D. E. MacLaughlin, J. Mag. Res. **30,** 483 (1978).
[8] J. M. Keartland, G. C. K. Fölscher, and M. J. R. Hoch, Phys. Rev. **B 43,** 8362 (1991).
[9] I. P. Goudemond, J. M. Keartland, and M. J. R. Hoch, J. Low Temp. Phys. **82,** 369 (1991).
[10] D. E. MacLaughlin, J. D. Williamson, and J. Butterworth, Phys. Rev. **B 4,** 60 (1971).
[11] A. P. Jeavons and G. A. Saunders, Proc. Roy. Soc. London **A 310,** 415 (1969).
[12] Ö. Öktü and G. A. Saunders, Proc. Phys. Soc. London **91,** 156 (1967).
[13] C. S. Ih and D. N. Langenberg, The Physics of Semimetals and Narrow Gap Semiconductors, Eds. D. E. Carter and R. T. Bate, Pergamon Press, Oxford 1971.
[14] L. R. Windmiller, Phys. Rev. **149,** 472 (1966).
[15] P. J. Lin and L. M. Falicov, Phys. Rev. **142,** 441 (1966).
[16] L. M. Falicov and P. J. Lin, Phys. Rev. **141,** 562 (1966).
[17] A. H. Mitchell, J. Chem. Phys. **26,** 1714 (1957).
[18] J. M. Keartland, G. C. K. Fölscher, and M. J. R. Hoch, to be submitted.
[19] F. Herman and S. Skillman, Atomic Structure Calculations, Prentice-Hall, Englewood Cliffs, New Jersey 1963.
[20] E. H. Hygh and T. P. Das, Phys. Rev. **143,** 452 (1966).
[21] A. Abragam, The Principles of Nuclear Magnetism, Oxford University Press, New York 1968.
[22] G. J. Hill, private communication.
[23] N. B. Brandt, N. Ya. Minina, and Yu. A. Pospelov, Sov. Phys. ETP **28,** 869 (1969).
[24] A. V. Rakhmanina, Sov. Phys. Solid State **22,** 403 (1980).
[25] Yu. A. Pospelov, JETP Lett. **33,** 82 (1981).